Performance Evaluation of Multicode Allocation System in WCDMA

Jui-Chi Chen
Institute of Computer Science
National Chung-Hsing University
250 Kuokuang Rd, Taichung 40227, Taiwan R.O.C.
rjchen@cs.nchu.edu.tw

Wen-Shyen E. Chen
Institute of Computer Science
National Chung-Hsing University
250 Kuokuang Rd, Taichung 40227, Taiwan R.O.C.
echen@cs.nchu.edu.tw

Abstract*-Few studies focused on the practical performance evaluation of OVSF multicode-allocation system in WCDMA. This paper proposes a model for evaluating the performance. From the model, we derive the expressions of call blocking probability and bandwidth utilization, both of which are two important performance measures in the system. Simulation results present that the measures seem to work. Subsequently, we apply the measures to solve a utilization optimization problem in consideration of network planning. As a consequence, the proposed model can approximately evaluate a multicode-allocation system, which should be useful for WCDMA networks.*

1. Introduction

Orthogonal variable spreading factor (OVSF) code transmission in Wideband-CDMA (WCDMA) supports a variety of wideband services from low to high data rates [1,2]. Both the forward and reverse links in WCDMA can apply only one OVSF code, single code, or multiple OVSF codes in parallel, multicode, to match the requested data rate by a user [2-9]. The OVSF codes are limited resources so that operators need to utilize them adequately. Call blocking probability (CBP) and bandwidth utilization (BU) are two important performance measures in the OVSF code-allocation systems, which represent the quality of service for subscribers and the profit of an operator, respectively. A code-allocation system can be defined as a 3G cell (there is one or few cells in a Node-B, the 3G base station).

In this paper we propose the queueing model $M^{\phi(x)}$/M/c/c to evaluate the performance of an OVSF multicode-allocation system. Single code-allocation system can be viewed as the multicode-allocation system with only one RAKE receiver (RAKE combiner). However, the model has just a linear number of states corresponding to the number of rate resources, which can be realized to solve its equilibrium equations. Finally, we apply the performance measures to solve a BU optimization problem, which can be considered in WCDMA network planning.

2. OVSF multicode-allocation system

In WCDMA, one spreading operation is the channelization that transforms each data symbol into a number of chips. The number of chips per data symbol is called spreading factor. The channelization codes are OVSF codes that preserve the orthogonality between channels of different rates. As shown in Fig. 1, a code tree recursively generates the OVSF codes based on a modified Walsh-Hadamard transformation [2]. $C^k_{ch,SF}$ represent the OVSF codes, where SF is the spreading factor of a code, k is the code number, and $1 \le k \le SF = 2^n$. The maximum spreading factor $SF_{\max}$ usually equals the system capacity. Without loss of generality, the data rates described later are normalized by the basic data rate R_b that represents an OVSF code with $SF_{\max}$.

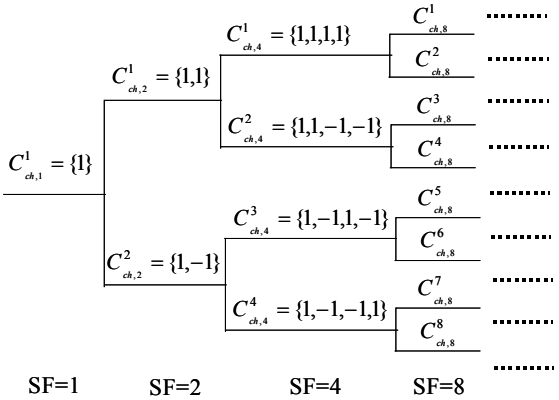

Fig. 1. Code tree for generation of the OVSF codes.

Generally, a request rate R_i for call i can be expressed in a polynomial as $R_i = \sum_{j=0}^{n} r_j * 2^j$, where $r_j \in \{0,1\}$, $n = \log_2(SF_{\max})$, $1 \le R_i \le SF_{\max}$, and R_i is the value of a multiplication of R_b. Then a user

equipment (UE) equipped with π RAKE receivers can convey only a multicode rate R_i with $\sum_{j=0}^{n} r_j \le \pi$. If a rate R_i with $\sum_{j=0}^{n} r_j > \pi$ is requested, then an approximate multicode allocation has to be performed. For example, the call i can be allocated with an approximate and slightly higher multicode rate limited in π codes, which can be expressed as $\phi(R_i, \pi)$

$$= \begin{cases} 0, \text{ if } \pi = 0 \text{ or } R_i = 0 \\ 2^{\lfloor \log_2(2R_i - 1) \rfloor}, \text{if } \pi = 1 \\ 2^{\lfloor \log_2(2R_i - 1) - 1 \rfloor} + \phi(R_i - 2^{\lfloor \log_2(2R_i - 1) - 1 \rfloor}, \pi - 1), \text{if } \pi \ge 2. \end{cases}$$

When $\pi = 1$, the approximate multicode rate forms an approximate single-code rate.

Before a code allocation, a cell has to check its available system capacity. In the code-limited test, the system capacity is equal to $SF_{\max} \cdot R_b$ in the cell. In fact, the cell may run out of the codes because the number of OVSF codes is limited. Then the new incoming calls in this moment will be blocked (rejected). CBP denotes the blocked probability of incoming call requests in a cell, regarded as the blocked calls divided by total calls during a long period of time. BU represents the utilized rate of total bandwidth in a cell, which can be defined by

$$\sum_{i=1}^{N} (T_{duration}^{i} \cdot \frac{SF_{\max}}{SF_i}) \Big/ (T_{total} \cdot SF_{\max}),$$

where N is the number of the successful calls during the total observing time T_{total}, and SF_i is the spreading factor of the i-th successful call with the duration $T_{duration}^{i}$.

3. Modeling

3.1. $M^{\phi(X)}$/M/c/c

In general, the number of OVSF codes with the maximum spreading factor $c = SF_{\max}$ is the system capacity in a cell, i.e., the cell has totally cR_b rate resources. The c basic-rate codes can be explained as parallel multiple servers to serve c channels simultaneously. Therefore, an OVSF multicode-allocation system can be seen as a multi-channel queue, having c servers in parallel, with batch arrival. A new call requesting kR_b, which will be allocated by an approximate multicode with $\phi(k)R_b$, can be seen as a group arrival with the size $\phi(k)$, where $\phi(k) = \phi(k, \pi)$. In the other aspect, a call served with $\phi(k)R_b$ can be viewed as $\phi(k)$ basic-rate codes released simultaneously. Assume that the customers arrive in groups following a Poisson process with the mean group arrival rate λ, and the service times (call holding times) are independently exponentially distributed with the parameter μ. Then the multicode system can be modeled on the batch-arrival model $M^{\phi(X)}$/M/c/c, which is a subset of M^{X}/M/c/c [10-12].

Fig. 2 depicts the state-transition-rate diagram of the model. Let the system support the variable rate ranging from 1 to $\phi(n)$. The arriving group size requested has a distribution $P(X = k) = x_k$, where $1 \le k \le n$. The average arriving group size $\bar{g} = \sum_{k=1}^{n} \phi(k) P(X = k) = \sum_{k=1}^{n} \phi(k) x_k$, where n is the maximum value that a call can request and results in the highest data rate $\phi(n)$ allocated. Let $\lambda_{\phi(k)}^{k}$ be the batch arrival rate with the request group size of Poisson user stream = k, where $\lambda_{\phi(k)}^{k} = x_k \lambda$, $\sum_{k=1}^{n} x_k = 1$, $1 \le k \le n \le \phi(n) \le c$, and $k, n \in N$. In Fig. 2 the dash lines denote other possible batch arrivals $\lambda_{\phi(k)}^{k}$. The model is equivalent to that on the single-code allocation system if $\pi = 1$.

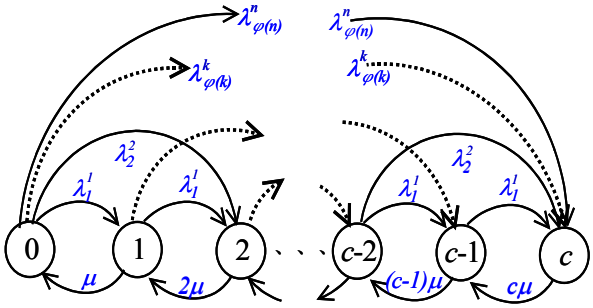

Fig. 2. State-transition-rate diagram for $M^{\phi(X)}$/M/c/c on an OVSF multicode-allocation system.

3.2. Equilibrium probabilities

To obtain the steady-state probability P_m for the model, we conduct its equilibrium equations as follows.

$\left(\sum_{k=1}^{n} \lambda_{\phi(k)}^{k}\right) P_0 = \mu P_1$, where $\sum_{k=1}^{n} \lambda_{\phi(k)}^{k} = \lambda$ and $1 \le n \le \phi(n) \le c$.

$$\left(m\mu + \sum_{k=1}^{\min[\phi^{-1}(c-m), n]} \lambda_{\phi(k)}^{k}\right) P_m = \sum_{k=1}^{\min[\phi^{-1}(m), n]} \lambda_{\phi(k)}^{k} P_{m-\phi(k)} + (m+1)\mu P_{m+1},$$

where $1 \le m \le c-1$ and $\phi^{-1}(m) = \phi^{-1}(m, \pi)$ is the maximum h so that $\phi(h, \pi) \le m$.

$c\mu P_c = \sum_{k=1}^{n} \lambda_{\phi(k)}^{k} P_{c-\phi(k)}$, which can be used for verification.

However, a recursive program cannot solve the equilibrium equations because of overabundant recursive levels for large c. Hence we use a computer-assist iterative procedure to solve the equations in the following.

Let $P_0^* = 1$; then $P_1^* = P_0^* (\lambda/\mu)$.

$$P_{m+1}^* = \left\{ \left(m\mu + \sum_{k=1}^{\min[\phi^{-1}(c-m),n]} \lambda_{\phi(k)}^k \right) P_m^* - \sum_{k=1}^{\min[\phi^{-1}(m),n]} \lambda_{\phi(k)}^k P_{m-\phi(k)}^* \right\} \Big/ (m+1)\mu$$

where $1 \le m \le c-1$.

According to the normalizing condition $\sum_{i=0}^{c} P_i = 1$, we finally have the equilibrium probabilities of all states:

$P_m = P_m^* \Big/ \sum_{i=0}^{c} P_i^*$, where $0 \le m \le c$.

4. Performance evaluation

4.1. Measures

Here two measures of the M$^{\phi(X)}$/M/c/c model, the CBP and BU, are evaluated for two cases in which the arriving group size requested has a discrete uniform distribution (DUNI) and a geometric distribution (GEOM). First, if a new call finds that the available capacity in the corresponding system cannot satisfy its rate requirement, it will be fully blocked. In other words, this is a batch-arrival batch-loss system. Thus the CBP in the system can be written as

$$\Omega = \sum_{i=0}^{\phi(n)-1} \left(P_{c-i} \sum_{k=\phi^{-1}(i)+1}^{n} \lambda_{\phi(k)}^k \Big/ \lambda \right),$$

where $1 \le k \le n \le \phi(n) \le c$, $c = SF_{\max}$, and $\pi \ge 1$.

The average number of customers in the system is $L_s = \sum_{i=0}^{c} iP_i$. It is equal to the mean number of busy servers in the system.

Observing the system for a long period of time T, we have the average BU written below.

$$\Psi = \lim_{T\to\infty} \frac{\sum_{k=1}^{n} \left[\lambda_{\phi(k)}^k T(1 - \sum_{i=c-\phi(k)+1}^{c} P_i) \cdot \phi(k) \cdot \frac{1}{\mu} \right]}{T \cdot c}$$

$$\text{by L' Hospital's rule} = \frac{\sum_{k=1}^{n} \left[\phi(k) \lambda_{\phi(k)}^k (1 - \sum_{i=c-\phi(k)+1}^{c} P_i) \right]}{c\mu},$$

where $\sum_{k=1}^{n} \left[\phi(k) \lambda_{\phi(k)}^k (1 - \sum_{i=c-\phi(k)+1}^{c} P_i) \right] = \bar{g}\lambda_{eff}$ and $1 \le n \le \phi(n) \le c$. There are $\lambda_{\phi(k)}^k T$ calls with $\phi(k)R_b$ incoming in the period T, then total $\lambda_{\phi(k)}^k T(1 - \sum_{i=c-\phi(k)+1}^{c} P_i)$ rate-$\phi(k)$ calls are served. Such rate-$\phi(k)$ bandwidth usage is $\lambda_{\phi(k)}^k T(1 - \sum_{i=c-\phi(k)+1}^{c} P_i) \cdot \phi(k) \cdot \frac{1}{\mu}$. Therefore, $\sum_{k=1}^{n} \left[\lambda_{\phi(k)}^k T(1 - \sum_{i=c-\phi(k)+1}^{c} P_i) \cdot \phi(k) \cdot \frac{1}{\mu} \right]$ is the total usage of all possible successful multicode users in the period T, where $1/\mu$ is the mean call holding time. Through the numerical analysis we can verify that $\Psi = L_s / c$.

Moreover, the average system waiting time can be shown as

$$W_s = \frac{L_s}{\bar{g}\lambda_{eff}} = L_s \Big/ \sum_{k=1}^{n} \left[\phi(k) \lambda_{\phi(k)}^k (1 - \sum_{i=c-\phi(k)+1}^{c} P_i) \right] = 1/\mu,$$

which follows Little's rule. [13]

4.2. Batch arrival with discrete uniform distribution

In comparison between theoretical and simulation results, the CBP and BU were calculated with μ = 0.00125 and λ ranging from 0.00625 to 0.075. To gain the good degree of correctness in the simulation, we adopted such small λ and μ. In this subsection, we consider that the group size requested is distributed with DUNI, where the maximum group size requested equals n, the maximum group size allocated is $\phi(n)$, and the average allocated group size is $\bar{g}$ (the normalized mean). Then the system has the traffic intensity $\rho = \bar{g}\lambda / c\mu$ and the offered load $\bar{g}\lambda / \mu$.

Fig. 3 indicates that both the CBP and the BU increases as ρ grows up, where n = 16, c = 128, π = 4, and $\bar{g}$ = 8.5. In addition, the figure shows that the theoretical results are close to those of the simulation. As a consequence, the proposed model seems to work for evaluating the multicode performance.

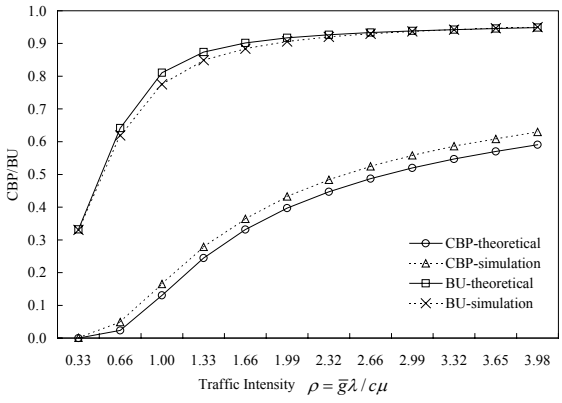

Fig. 3. Comparison between theoritical and simulation results in consideration of CBP and BU.

Similarly, Table 1 presents another approximate result between the theoretical analysis and the simulation, where n = 16, c = 32, π = 2, and $\bar{g}$ = 9.

Table 1. Comparison between theoretical and simulation results using DUNI arrival-group distribution.

	CBP		BU	
ρ	theoretical	simulation	theoretical	simulation
1.4	0.3753109	0.4196958	0.6526834	0.6455787
2.8	0.5410689	0.5867507	0.7580674	0.7690922
4.2	0.6222220	0.6666620	0.8038209	0.8213842
5.6	0.6726803	0.7150725	0.8312586	0.8500467
7.0	0.7079357	0.7466269	0.8500972	0.8685577
8.4	0.7343755	0.7715199	0.8640941	0.8817360
9.8	0.7551810	0.7898847	0.8750512	0.8921705
11.3	0.7721299	0.8051404	0.8839487	0.9007946
12.7	0.7862991	0.8173375	0.8913694	0.9068861
14.1	0.7983831	0.8268297	0.8976847	0.9123287
15.5	0.8088525	0.8360114	0.9031449	0.9169757
16.9	0.8180397	0.8442116	0.9079262	0.9208874

4.3. Batch arrival with geometric distribution

In fact, one can apply any countable distributions, e.g., constant, discrete uniform, and geometric distributions, for mapping the behavior of the arriving group size. In this subsection we consider that the group size requested is distributed with GEOM, λ varies from 0.00625 to 0.075, and μ = 0.00125.

Table 2 lists the normalized probability of GEOM P_k ranging from P_1 to P_{16} because of n = 16, the multicode mapping from the request group size k to the allocated (served) group size $\phi(k)$, and the different values of $\bar{g}$ with accordance to various π.

Table 2. The normalized probability of GEOM P_k and the multicode mapping from k to $\phi(k)$.

	GEOM	π=1		π=2		π=3	
k	P_k	$\phi(k)$	$\phi(k)*P_k$	$\phi(k)$	$\phi(k)*P_k$	$\phi(k)$	$\phi(k)*P_k$
1	0.18899	1	0.18899	1	0.18899	1	0.18899
2	0.15475	2	0.30949	2	0.30949	2	0.30949
3	0.12663	4	0.50652	3	0.37989	3	0.37989
4	0.10372	4	0.41488	4	0.41488	4	0.41488
5	0.08486	8	0.67892	5	0.42432	5	0.42432
6	0.06949	8	0.55592	6	0.41694	6	0.41694
7	0.05698	8	0.45581	8	0.45581	7	0.39883
8	0.04659	8	0.37271	8	0.37271	8	0.37271
9	0.03812	16	0.61000	9	0.34312	9	0.34312
10	0.03127	16	0.50039	10	0.31274	10	0.31274
11	0.02558	16	0.40935	12	0.30702	11	0.28143
12	0.02094	16	0.33506	12	0.25129	12	0.25129
13	0.01713	16	0.27407	16	0.27407	13	0.22268
14	0.01404	16	0.22464	16	0.22464	14	0.19656
15	0.01149	16	0.18384	16	0.18384	16	0.18384
16	0.00941	16	0.15058	16	0.15058	16	0.15058
Σ	4.83682	$\bar{g}$	6.17116	$\bar{g}$	5.01034	$\bar{g}$	4.84831

Table 3 presents another approximate result between the theoretical analysis and the simulation using GEOM arrival-group distribution, where n = 16, c = 64, π = 3, and $\bar{g}$ = 4.84831. The result shows that the theoretical analysis has good approximate values as that the simulation does.

Table 3. Comparison between theoretical and simulation results using GEOM arrival-group distribution.

	CBP		BU	
ρ	theoretical	simulation	theoretical	simulation
0.38	0.0019395	0.0073788	0.3771463	0.3651531
0.76	0.0549930	0.0814978	0.6747268	0.6394210
1.14	0.1571313	0.1903232	0.8072016	0.7763178
1.52	0.2474997	0.2835579	0.8628169	0.8415415
1.89	0.3186507	0.3567943	0.8916074	0.8786045
2.27	0.3751914	0.4134495	0.9092223	0.9006256
2.65	0.4212449	0.4595864	0.9212304	0.9155875
3.03	0.4596228	0.4969547	0.9300201	0.9259404
3.41	0.4922173	0.5286403	0.9367791	0.9341334
3.79	0.5203355	0.5555008	0.9421667	0.9404891
4.17	0.5449080	0.5793255	0.9465797	0.9455824
4.55	0.5666164	0.5984197	0.9502728	0.9495795

Accordingly, given c = 256, π = 3, and $\bar{g}$ = 4.84831, Table 4 compares the other theoretical measures with the simulation, including the theoretical BU Ψ, the theoretical BU L_s/c, the average number of busy servers L_s, and the average system delay W_s.

Table 4. Comparison of some measures between theoretical and simulation results using GEOM arrival-group distribution

			Simu.		Simu.	$1/\mu$	Simu.
ρ	Ψ	L_s/c	BU	L_s	L_s	W_s	W_s
0.0947	0.0947	0.0947	0.0929	24.2	23.8	800	800.2
0.1894	0.1894	0.1894	0.1846	48.5	47.2	800	797.9
0.2841	0.2841	0.2841	0.2766	72.7	70.8	800	799.2
0.3788	0.3788	0.3788	0.3675	97.0	94.0	800	799.6
0.4735	0.4735	0.4735	0.4578	121.2	117.1	800	799.8
0.5682	0.5681	0.5681	0.5472	145.4	140.0	800	799.6
0.6629	0.6618	0.6618	0.6337	169.4	162.1	800	798.5
0.7575	0.7495	0.7495	0.7114	191.9	182.0	800	797.7
0.8522	0.8210	0.8210	0.7791	210.2	199.3	800	798.5
0.9469	0.8708	0.8708	0.8294	222.9	212.2	800	798.3
1.0416	0.9028	0.9028	0.8645	231.1	221.2	800	799.3
1.1363	0.9231	0.9231	0.8930	236.3	228.5	800	799.1

5. An application

In this section, we examine an application with the performance measures -- an optimization problem that finds the optimal number of basic-rate codes in a cell for maximizing the BU with a given CBP constraint. The optimization problem can be described in the following.

Given λ, μ, and a CBP constraint C_{Pc}, determine the optimal value of c so as to

$$\text{Maximize} \quad \frac{\sum_{k=1}^{n}\left[\phi(k)\lambda_{\phi(k)}^{k}(1-\sum_{i=c-\phi(k)+1}^{c}P_i)\right]}{c\mu}$$

$$\text{Subject to} \quad \lambda > 0,\ \mu > 0, \text{ and } 1 > C_{Pc} > 0$$

$$\Omega = \sum_{i=0}^{\phi(n)-1}\left(P_{c-i}\sum_{k=\phi^{-1}(i)+1}^{n}\lambda_{\phi(k)}^{k}\Big/\lambda\right) \le C_{Pc},\ c \in N.$$

To verify the monotonicity of the CBP and BU in a system, we traced them by numerical analysis, as shown in Fig. 4, where the group size requested is distributed with DUNI, $\bar{g}$ = 8.5625, n = 16, π = 3, λ = 0.00625, μ = 0.00125, and the offered load is $\bar{g}\lambda/\mu$ = 42.8125. Under the constant offered load, the higher c is, the lower the CBP becomes. Nevertheless, the BU may not have the monotonicity under certain offered load such as 42.8125. As a result, solving the optimization problem means that first determine c for maximizing the CBP restricted by C_{Pc}, then search for possible larger c so that the BU is maximized.

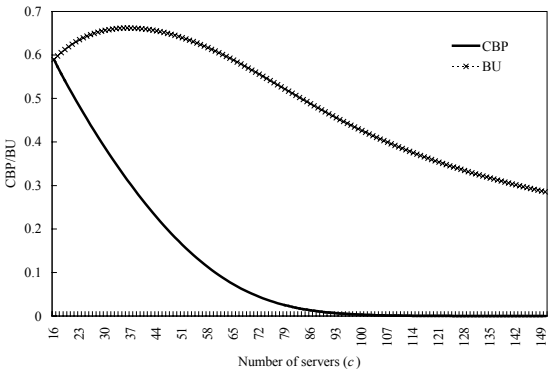

Fig. 4. The presentation of the CBP and BU in a system as the number of servers c grows up (offered load = 42.8125).

Table 5 presents each optimal c in various offered load and the corresponding BU optimized, where n = 16, Cp_c = 3%, μ = 0.00125, λ ranges from 0.00625 to 0.05, π varies from 1 to 3 ($\bar{g}$ = 6.17, 5.01, and 4.85, respectively), and the group size requested is distributed with GEOM. The case of the optimal c plus one reduces the BU. On the other hand, the CBP exceeds the constraint C_{Pc} in the case of the optimal c minus one, while the BU decreases in the case of the optimal c plus one. This explains that the values of c presented in the table are the optimal ones.

In OVSF code-allocation systems, the optimal c for maximizing BU can be considered for setting about c basic-rate codes in the corresponding cell. That is, the cell should be assigned the corresponding frequency bandwidth for supporting the c codes.

Table 5. The optimal values of c for maximizing BU with CBP ≤ 3% (Cp_c = 3%) in various offered load.

offer load	π	Opt. c	CBP [c-1]	CBP [c]	BU [c-1]	BU [c]	BU [c+1]
31	1	58	0.0327	0.0299	0.5030	0.4975	0.4920
62	1	92	0.0317	0.0297	0.6327	0.6285	0.6244
123	1	156	0.0311	0.0298	0.7448	0.7421	0.7395
185	1	218	0.0309	0.0298	0.7989	0.7970	0.7951
247	1	279	0.0307	0.0299	0.8320	0.8305	0.8290
25	2	47	0.0327	0.0293	0.5054	0.4985	0.4917
50	2	75	0.0308	0.0284	0.6327	0.6276	0.6223
100	2	127	0.0306	0.0290	0.7450	0.7416	0.7383
150	2	177	0.0310	0.0297	0.8000	0.7976	0.7952
200	2	227	0.0304	0.0294	0.8320	0.8302	0.8283
24	3	46	0.0303	0.0268	0.5045	0.4972	0.4899
49	3	72	0.0322	0.0296	0.6384	0.6329	0.6274
97	3	123	0.0306	0.0289	0.7467	0.7432	0.7397
145	3	172	0.0304	0.0291	0.8000	0.7975	0.7949
194	3	220	0.0305	0.0294	0.8330	0.8311	0.8291

6. Concluding remarks

We have proposed a batch-arrival model for evaluating the CBP and BU in an OVSF multicode-allocation system, two important performance measures. The simulation results agree with the predictions derived from the theoretical model. Furthermore, we applied the measures to solve the BU optimization problem. The proposed model, however, can approximately evaluate the system, which should be useful for WCDMA networks.

7. References

[1] F. Adachi, M. Sawahashi, and H. Suda, "Wideband CDMA for next generation mobile communications systems," *IEEE Commun. Mag.*, vol. 36, no. 9, pp. 56-69, Sep. 1998.

[2] *3GPP Technical Specification 25.213, v5.1.0, Spreading and modulation (FDD) (Release 5)*, June 2002.

[3] E. H. Dinan and B. Jabbari, "Spreading codes for direct sequence CDMA and wideband CDMA cellular networks," *IEEE Commun. Mag.*, pp. 48-54, Sep. 1998.

[4] S. J. Lee, H. W. Lee, and D. K. Sung, "Capacities of single-code and multicode DS-CDMA systems accommodating multiclass services," *IEEE Trans. on Vehicular Tech.*, vol. 48, no. 2, pp. 376-384, Mar. 1999.

[5] Y. Yang and T. P. Yum, "Maximally flexible assignment of orthogonal variable spreading factor codes for multirate traffic," *IEEE Trans.*

on Wireless Commun., vol. 3, no. 3, pp. 781-792, May 2004.

[6] A. N. Rouskas, D. N. Skoutas, G. T. Kormentzas, and D. D. Vergados, "Code reservation schemes at the forward link in WCDMA," *Computer Commun.*, vol. 27, pp. 792-800, 2004.

[7] L. Yen and M. Tsou, "An OVSF code assignment scheme utilizing multiple Rake combiners for W-CDMA," in *Proc. of IEEE ICC'03*, pp. 3312-3316, 2003.

[8] Y. C. Tseng and C. M. Chao, "Code placement and replacement strategies for wideband CDMA OVSF code tree management," *IEEE Trans. on Mobile Computing*, vol. 1, no. 4, pp. 293-302, Oct.-Dec. 2001.

[9] S. Ramakrishna and J. M. Holtzman, "A comparison between single code and multiple code transmission schemes in a CDMA system," in *Proc. of IEEE VTC'98*, pp. 791-795, May 1998.

[10] M. V. Cromie, M. L. Chaudhry, and W. K. Grassmann, "Further results for the queueing system M^X/M/c," *Journal of the Operational Research Society*, vol. 30, no. 8, pp. 755-763, 1979.

[11] L. M. Abol'nikov and R. M. Yasnogoridskiy, "Investigation of many channel nonstationary Markov systems with non-ordinary input flow," *Engineering Cybernetics*, vol. 10, pp. 636-642, 1972.

[12] I. W. Kabak, "Blocking and delays in $M^{(x)}$/M/c bulk arrival queueing systems," *Management Science*, vol. 17, pp. 112-115, 1970.

[13] M. L. Chaudhry, U. C. Gupta, and V. Goswami, "Modeling and analysis of discrete-time multiserver queues with batch arrivals: GI^X/Geom/m," *Journal on Computing*, vol. 13, no. 3, pp. 172-180, 2001.